

High fidelity one-qubit operations under random telegraph noise

Mikko Möttönen*

*Department of Chemistry and Pitzer Center for Theoretical Chemistry,
University of California, Berkeley, CA 94720 and
Laboratory of Physics, Helsinki University of Technology
P. O. Box 1100, FIN-02015 HUT, Finland*

Rogério de Sousa, Jun Zhang, and K. Birgitta Whaley
*Department of Chemistry and Pitzer Center for Theoretical Chemistry,
University of California, Berkeley, CA 94720*

(Dated: October 31, 2018)

We address the problem of implementing high fidelity one-qubit operations subject to time dependent noise in the qubit energy splitting. We show with explicit numerical results that high fidelity bit flips and one-qubit NOT gates may be generated by imposing bounded control fields. For noise correlation times shorter than the time for a π -pulse, the time optimal π -pulse yields the highest fidelity. For very long correlation times, fidelity loss is approximately due to systematic error, which is efficiently tackled by compensation for off-resonance with a pulse sequence (CORPSE). For intermediate ranges of the noise correlation time we find that short CORPSE, which is less accurate than CORPSE in correcting systematic errors, yields higher fidelities. Numerical optimization of the pulse sequences using gradient ascent pulse engineering results in noticeable improvement of the fidelities for the bit flip and marginal improvement for the NOT gate.

I. INTRODUCTION

In physical implementations of quantum computers, one of the most challenging tasks is to find an efficient and experimentally feasible way to overcome the problems caused by undesired interactions between the quantum bits, qubits, and their surrounding environment. These interactions, which destroy the quantum interference between qubit states, lead to errors and loss of fidelity, a phenomenon generally referred to as decoherence.

A variety of methods to fight decoherence have been proposed in the literature, including error correcting codes [1, 2], decoherence free subspace coding [3, 4], noiseless subsystem coding [5], dynamical decoupling [6, 7, 8], quantum feedback control [9, 10], and quantum reservoir engineering [11]. Most of these schemes are not efficient in making full use of all the physical resources. For example, encoding schemes employing decoherence free subspaces or error correcting codes store the quantum information in a specific portion of the whole qubit space, or encode several physical qubits into one logical qubit. Design and applicability of such codes depends on the nature of the decoherence sources and imposes additional requirements on encoding and decoding. Dynamical decoupling schemes possess the attractive feature that they require no ancillary qubits, since the interactions between the qubits and the environment are effectively canceled out by applying external control fields. It has also been shown that such decoupling can be realized us-

ing finite energy soft pulses [8], and that it is possible to carry out qubit rotations without disturbing the decoupling process [7]. However, dynamical decoupling is based on stroboscopic pulsing of the qubit, at a rate significantly faster than the usual characteristic frequency of environmental fluctuations. This requires strong control fields, which might cause technical problems in the laboratory. For example, it has been pointed out that the high energy deposition needed for dynamical decoupling of nuclear spins is incompatible with the low temperature requirement in some qubit implementations [12].

In this paper, we consider the design of fidelity optimized one-qubit operations in a noisy environment. Motivated by experiments in solid state qubits [13, 14], we assume random telegraph noise (RTN) [15] in the qubit energy splitting as a phenomenological model for the environmental fluctuations. Whereas an ensemble of RTN fluctuators models the ubiquitous $1/f$ noise in electronic circuits [16], solid state devices on the nanoscale are often found to be affected by a single RTN source [17, 18] characterized by its correlation time τ_c . Although we assume that the noise couples only to the qubit energy splitting, a similar analysis can be made for errors in the rotation angle [19, 20].

Composite pulses are known to provide an efficient way to reduce errors due to systematic off-resonant perturbations, e.g., compensation for off-resonance with a pulse sequence (CORPSE) [21]. Here we focus on the situation in which the perturbation of a qubit is fluctuating in time, and seek to suppress the decoherence arising from this time-dependent noise by imposition of a bounded control field. We are particularly interested in the regime where the maximal energy a_{\max} pro-

*Electronic address: mikko.mottonen@tkk.fi

vided by the control field is related to the noise correlation time as $\tau_c a_{\max}/\hbar \sim 1$, since this is an important regime for the experimentalists where dynamical decoupling is not applicable. In this regime, we find that a novel optimized pulse profile can increase the fidelity of quantum operations by up to 30% in comparison to the standard composite pulse sequences such as CORPSE and short CORPSE (SCORPSE) [21, 22]. However, we provide an analysis over the entire range of correlation times, ranging from short noise correlation times satisfying $\tau_c a_{\max}/\hbar \ll 1$, where the optimal fidelity is obtained by pulsing at minimum time, to the long correlation time regime, $\tau_c a_{\max}/\hbar \gg 1$, where to a good approximation, the fidelity loss is due to systematic time-independent errors. The latter case is efficiently tackled by the composite pulse approach [21, 22].

It was stated in Ref. [22] that CORPSE is the shortest sequence in the family of composite pulse sequences correcting systematic errors as efficiently as possible and composing of up to three pulses. Therefore, it was considered to be the most useful one. Whereas SCORPSE is not as accurate as CORPSE, it is shorter in time. Thus it may still be of some interest, depending on the physical scenario. We illustrate this fact here by showing that SCORPSE actually yields higher fidelities than CORPSE in the regime of intermediate noise correlation time, $\tau_c a_{\max}/\hbar \sim 1$, for the one-qubit example studied here. The optimal performance of CORPSE is in fact limited to just the long correlation time regime. We also go beyond these composite pulse sequences to obtain fidelity optimized pulses consisting of large numbers of pulse amplitudes that are numerically derived using an adaptation of the method of gradient ascent pulse engineering (GRAPE) [23]. Although GRAPE was originally developed for finding control pulses in closed quantum systems, it is utilized here to the determination of bounded control pulses in a noisy quantum system. We find that numerical optimization of a pulse sequence with GRAPE noticeably increases the fidelity of bit flip operations, compared with the results of the standard composite pulse sequences. In contrast to this improvement for a bit flip, only a rather marginal improvement in fidelity is found on employing GRAPE to numerically generate a fidelity-optimized control pulse sequence for the complete one-qubit NOT gate.

The remainder of this paper is organized as follows. In Sec. II, we characterize the system Hamiltonian, the noise model, and the fidelity. Section III introduces the pulse sequence generation methods we use for the noisy qubit system, and Sec. IV presents the results obtained for implementation of a state transformation corresponding to a bit flip and a quantum gate corresponding to the one-qubit NOT gate. Finally, Sec. V concludes the paper with a discussion of extensions and possible generalizations.

II. SYSTEM CHARACTERIZATION

We consider a single qubit described by the effective Hamiltonian

$$H = \sum_{i \in \{x, y, z\}} [a_i(t) + \eta_i(t)] \sigma_i, \quad (1)$$

where the symbols $\{\sigma_i\}$ denote the Pauli spin matrices [24], $\{\eta_i(t)\}$ are the amplitudes of the environmental noise, and $\{a_i(t)\}$ are the external control fields. Note that the latter are parameterized here by their corresponding energy amplitudes, rather than the actual physical control fields, e.g., electric field amplitudes. We assume that the strength of the control fields is finite, and denote their maximum possible value by a_{\max} . To simplify the discussion, we consider only the case when there is no control in the y or z directions, and no noise in the x and y directions. Under these assumptions, the Hamiltonian becomes

$$H = a(t)\sigma_x + \eta(t)\sigma_z, \quad (2)$$

where the control field $a := a_x \in [-a_{\max}, a_{\max}]$ and we have used the notation $\eta(t) := \eta_z(t)$.

For RTN, the amplitude of the noise η changes randomly in time between two values $-\Delta$ and Δ . The quantity Δ describes the strength of the noise, and the frequency of the jumps between $-\Delta$ and Δ is determined by the correlation time τ_c . Specifically, the probability of the noise to jump in an infinitesimal time interval dt is given by $\frac{dt}{\tau_c}$. Hence, the probability of no jumps taking place in a time interval of length t is

$$p_0(t) = e^{-t/\tau_c}. \quad (3)$$

In generating sample trajectories of RTN, Eq. (3) can also be inverted to yield the sojourn time before a jump takes place. Thus we get a sample trajectory of RTN by taking random numbers $p_i \in (0, 1)$ and then deriving the corresponding jump time instants

$$t_i = \sum_{j=1}^i -\tau_c \ln(p_j). \quad (4)$$

Using the values of these jump times, we can express the noise process $\eta(t)$ as

$$\eta(t) = (-1)^{\sum_i \Theta(t-t_i)} \eta(0), \quad (5)$$

where $\Theta(t)$ is the Heaviside step function.

Since we use an effective Hamiltonian operating solely on the qubit rather than treating the full quantum dynamics of both the qubit and the environment, we need to average over different noise trajectories in order to obtain the system dynamics under the influence of RTN. Therefore, the dynamics of the system density matrix ρ can be written as

$$\rho(t) = \lim_{N \rightarrow \infty} \frac{1}{N} \sum_{k=1}^N U_k \rho_0 U_k^\dagger, \quad (6)$$

where $\rho_0 = \rho(0)$ is the initial state of the system and the operators $\{U_k\}$ refer to unitary time evolution of the system under a certain trajectory $\eta_k(t)$. Formally, the operator $\{U_k\}$ is written as

$$U_k = \mathcal{T} e^{-i \int_0^t d\tau [a(\tau)\sigma_x + \eta_k(\tau)\sigma_z]/\hbar}, \quad (7)$$

where \mathcal{T} is the time ordering operator.

Let ρ_f be the desired final state of the system. Following Ref. [23], we define the fidelity function as

$$\phi(\rho_f, \rho_0) = \text{tr}\{\rho_f^\dagger \rho(T)\}, \quad (8)$$

where $\rho(T)$ is the actual state of the system at the final time instant T . Substituting Eq. (6) into Eq. (8), we obtain

$$\phi(\rho_f, \rho_0) = \lim_{N \rightarrow \infty} \frac{1}{N} \sum_{k=1}^N \text{tr}\{\rho_f^\dagger U_k \rho_0 U_k^\dagger\}. \quad (9)$$

Equation (9) shows that the fidelity function defined here can be viewed as an average over fidelity functions corresponding to individual unitary time developments in noiseless quantum systems that are characterized by the evolution operators U_k .

Let us write the initial state of the qubit as

$$\rho_0 = (I + c_x \sigma_x + c_y \sigma_y + c_z \sigma_z)/2, \quad (10)$$

where c_i are real numbers. For implementation of quantum gates rather than state transformations, we define a fidelity function as the average over all pure initial conditions of the qubit:

$$\Phi(U_f) = \frac{1}{4\pi} \int_{c_x^2 + c_y^2 + c_z^2 = 1} d\Omega \phi(U_f \rho_0 U_f^\dagger, \rho_0), \quad (11)$$

where the operator that we desire to implement is denoted by U_f and $d\Omega$ is an infinitesimal solid angle on the Bloch sphere. Simplification of the integral in Eq. (11) yields

$$\Phi(U_f) = \frac{1}{2} + \lim_{N \rightarrow \infty} \frac{1}{12N} \sum_{k=1}^N \sum_{j=1}^3 \text{tr}\{U_f \sigma_j U_f^\dagger U_k \sigma_j U_k^\dagger\}. \quad (12)$$

III. PULSE SEQUENCES FOR NOISY SYSTEMS

In this section, we introduce the pulse sequences that will be used for suppression of decoherence. We first summarize the two composite pulse sequences CORPSE and SCORPSE [21, 22] that were originally designed to correct systematic errors in the implementation of one-qubit quantum gates. The control fields corresponding to the CORPSE pulse sequence are

$$a_C(t) = \begin{cases} a_{\max}, & \text{for } 0 < t' < \pi/3 \\ -a_{\max}, & \text{for } \pi/3 \leq t' \leq 2\pi \\ a_{\max}, & \text{for } 2\pi < t' < 13\pi/3, \end{cases} \quad (13)$$

where t is related to the dimensionless time t' by $t' = a_{\max} t/\hbar$. For the SCORPSE pulse sequence we have the control fields

$$a_{\text{SC}}(t) = \begin{cases} -a_{\max}, & \text{for } 0 < t' < \pi/3 \\ a_{\max}, & \text{for } \pi/3 \leq t' \leq 2\pi \\ -a_{\max}, & \text{for } 2\pi < t' < 7\pi/3. \end{cases} \quad (14)$$

In the absence of noise, the CORPSE and SCORPSE pulse sequences generate both the one-qubit NOT gate and the bit flip state transformation.

An alternative to these composite pulse sequences is provided by numerical construction of pulse sequences optimized for maximum fidelity. Such fidelity-optimized sequences may be constructed by an adaptation of the GRAPE algorithm [23] which was originally designed to steer the dynamics of coupled nuclear spins. No noise effects or bounds on control fields are included in the original implementation. For full details of the GRAPE algorithm for closed quantum systems, see Ref. [23].

The key feature of the GRAPE algorithm is to approximate the continuous pulse shape on a time interval $[0, T]$ by a function that is constant on n small time intervals of length $\Delta t = T/n$, and then to derive the corresponding gradients of the fidelity function with respect to these constant values. Let U_k^m be the unitary time evolution operator corresponding to the time interval $[(m-1)\Delta t, m\Delta t]$ and to the noise trajectory η_k . In this interval, the control field is approximated by a constant, a^m . Since the fidelity function $\phi(\rho_f, \rho_0)$ is an average of the fidelity functions used in Ref. [23], the gradient of $\phi(\rho_f, \rho_0)$ is obtained as an average of the gradients derived in Ref. [23]. Thus

$$\frac{\delta \phi(\rho_f, \rho_0)}{\delta a^m} = -\frac{i\Delta t}{\hbar} \lim_{N \rightarrow \infty} \frac{1}{N} \sum_{k=1}^N \text{tr}\{(\lambda_k^m)^\dagger [\sigma_x, \rho_k^m]\}, \quad (15)$$

where

$$\lambda_k^m = (U_k^n U_k^{n-1} \dots U_k^{m+1})^\dagger \rho_f U_k^n U_k^{n-1} \dots U_k^{m+1}, \quad (16)$$

and

$$\rho_k^m = U_k^m U_k^{m-1} \dots U_k^1 \rho_0 (U_k^m U_k^{m-1} \dots U_k^1)^\dagger. \quad (17)$$

In the case that there exist other control terms $\{a_k^c(t) H_k^c\}$ in the Hamiltonian, the corresponding gradients can be obtained from Eq. (15) by substituting a by a_k^c and σ_x by H_k^c .

We note that for $\Delta = 0$, all the individual RTN trajectories are identical and consequently the averaging and limiting procedures in Eq. (15) can be omitted. In this case, Eq. (15) reduces to the equation for noiseless systems derived in Ref. [23].

To derive the gradient of the average fidelity Φ , we note that

$$\Phi(U_f) = \frac{1}{2} + \frac{1}{12} \sum_{j=1}^3 \phi(U_f \sigma_j U_f^\dagger, \sigma_j). \quad (18)$$

Hence, the gradient of Eq. (18) can be obtained from Eq. (15) as

$$\frac{\delta\Phi(U_f)}{\delta a^m} = \frac{1}{12} \sum_{j=1}^3 \frac{\delta\phi(U_f \sigma_j U_f^\dagger, \sigma_j)}{\delta a^m}. \quad (19)$$

In the GRAPE algorithm, we calculate the gradient of the desired fidelity function using Eq. (15) or (19), and update the control fields by moving along the direction of the gradient with the restriction $a \in [-a_{\max}, a_{\max}]$. This procedure results in an optimized pulse sequence for a given operation time T . Moreover, the fidelity is also optimized with respect to the operation time.

We note that the pulse sequences yielding the optimal fidelity for each set of system parameters are not unique. In order to find as smooth and as simple sequence as possible, we therefore start from a constant control field and use the gradient method to maximize the fidelity. To ascertain whether our solution achieves a local or the global maximum in fidelity, we repeated the procedure for several different, uncorrelated initial values of the control field. This resulted in different pulse sequences with equal fidelities, suggesting that we have indeed found the global maximum, though this cannot be conclusively claimed. Thus, when we refer to the results of the GRAPE algorithm, we shall describe the corresponding pulse sequences as optimized rather than optimal.

IV. HIGH FIDELITY ONE-QUBIT OPERATIONS

In this section, we present optimized pulse sequences implementing high fidelity one-qubit operations that were obtained using the GRAPE algorithm, and compare the results with those from the standard CORPSE and SCORPSE pulse sequences. We restrict our attention here to two quantum operations on the one-qubit system, namely, the state transformation corresponding to a bit flip, and the one-qubit NOT gate.

A. Bit flip

We consider a one-qubit bit flip, i.e., flipping a one-qubit state from one of the two poles of the Bloch sphere to the other. This problem may arise, for example, when some qubits of a multi-qubit register need to be flipped to reach a non-trivial state after a collective initialization. The initial and final states can be taken as

$$\rho_0 = \begin{pmatrix} 0 & 0 \\ 0 & 1 \end{pmatrix} \quad \text{and} \quad \rho_f = \begin{pmatrix} 1 & 0 \\ 0 & 0 \end{pmatrix}. \quad (20)$$

We first consider the limiting cases: vanishing noise correlation time, and infinite noise correlation time.

Case 1: $\tau_c \rightarrow 0$. In this case, RTN averages out due to the well-known phenomenon of motional narrowing [25]

since the noise changes its sign so rapidly that there is no time for the qubit to drift into the direction of the noise at any given time. It is therefore not surprising that a time optimal π -pulse

$$a_\pi(t) = a_{\max}, \quad \text{for } t \in [0, \pi\hbar/a_{\max}], \quad (21)$$

is also fidelity optimal, since it is impossible to correct arbitrary fast switching using bounded controls.

Case 2: $\tau_c \rightarrow \infty$. In this limiting case, RTN reduces to a constant drift, whereas for large but finite τ_c the drift may be treated as approximately constant. In comparison to a π -pulse, pulse sequences such as CORPSE and SCORPSE that are specifically designed to correct systematic errors will clearly improve the fidelity of the desired quantum operation here.

In Fig. 1, the fidelities obtained from π -pulse, CORPSE, SCORPSE, and GRAPE pulse sequences for a bit flip are plotted as functions of the correlation time τ_c . The noise strength Δ is chosen to be $0.125 \times a_{\max}$ in this example. As expected, GRAPE yields the highest fidelities for all values of noise correlation time τ_c since it enforces optimization of the pulse sequence. Note that the fidelity curve of GRAPE has a global minimum near the correlation time $\tau_c \approx 3\hbar/a_{\max}$. The existence of the minimum is due to the fact that since the GRAPE pulse sequences are optimized, they will not only yield perfect unit fidelity in the short correlation time limit $\tau_c \rightarrow 0$ as a result of motional narrowing, but they will also yield unit fidelity in the long correlation time limit $\tau_c \rightarrow \infty$. The latter argument is true since small systematic errors can be corrected to arbitrary accuracy [26] and provided that the GRAPE algorithm does find the global optimal solution. Consequently, there must be a minimum at a finite value of τ_c in the fidelity curve generated by GRAPE. The corresponding fidelity curves of the CORPSE and the SCORPSE pulse sequences also show such minima which result from the fact that these sequences are specifically designed to correct the systematic errors. In contrast, the fidelity curve for the π -pulse is seen to be a monotonically decreasing function of the correlation time, reflecting the fact that this pulse cannot correct systematic errors. Figure 1 also provides a good example of the general result that for intermediate noise correlation times SCORPSE is more favorable than CORPSE. This is a consequence of the shorter operation time of SCORPSE, which is more significant at finite values of τ_c than the fact that CORPSE is more efficient than SCORPSE in correcting systematic errors. This balance between the length of the operation time and the accuracy in correcting systematic errors results in a cross-over between the fidelity curves of SCORPSE and CORPSE at very large correlation times. Hence, the CORPSE curve eventually rises above the SCORPSE curve for longer τ_c than shown in Fig. 1.

As discussed in Sec. III, the GRAPE algorithm for finding optimal pulse sequences involves optimization of the operation time T . However, the RTN used in this work does not have any dynamical effect on the initial

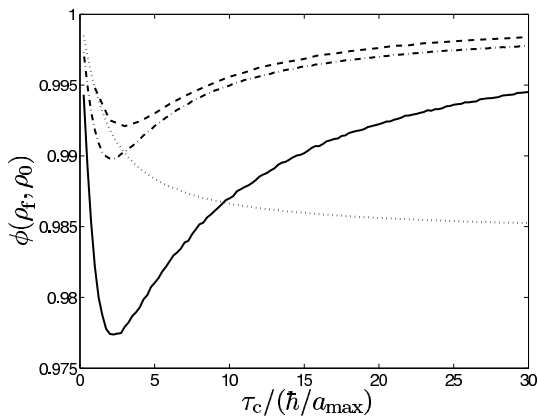


FIG. 1: Fidelities $\phi(\rho_f, \rho_0)$ as functions of the noise correlation time τ_c for a π -pulse (Eq. (21), dotted line), CORPSE (Eq. (13), solid line), and SCORPSE (Eq. (14), dash-dotted line). The optimized fidelity found using GRAPE is shown as the dashed line. The strength of the RTN in this example is $\Delta = 0.125 \times a_{\max}$.

density matrix ρ_0 . Moreover, the noise is Markovian and hence any pulse $a'(t)$ with operation time $T' < T$ may be extended to an operation time T without change of fidelity by setting

$$a(t) = \begin{cases} 0, & \text{for } 0 < t < T - T' \\ a'(t - T + T'), & \text{for } T - T' < t < T. \end{cases} \quad (22)$$

Thus the fidelity is a monotonically increasing function of the operation time T . In fact, it is found that the fidelity saturates at a maximum value for rather short operation times, see for example Fig. 2.

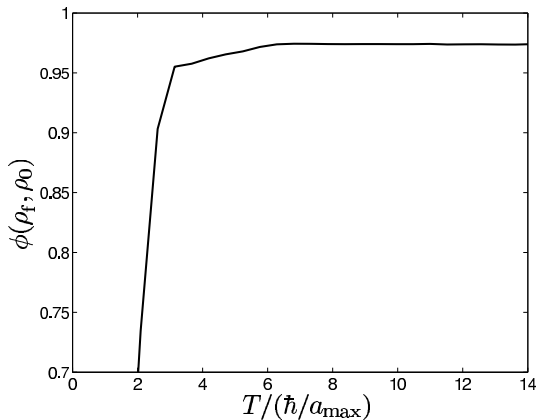


FIG. 2: Fidelity $\phi(\rho_f, \rho_0)$ of the GRAPE pulse sequence as a function of the operation time T , for noise correlation time $\tau_c = 5\hbar/a_{\max}$ and noise strength $\Delta = 0.25 \times a_{\max}$.

Figure 3 shows the error $\epsilon(\rho_f, \rho_0) = 1 - \phi(\rho_f, \rho_0)$ of the GRAPE optimized result as a function of the correlation time τ_c , for several different noise strengths. A quadratic dependence of the error on the noise strength, $\epsilon \propto \Delta^2$, is observed over the parameter ranges $\Delta \in [a_{\max}/16, a_{\max}/4]$ and $\tau_c \in [0, 30\hbar/a_{\max}]$.

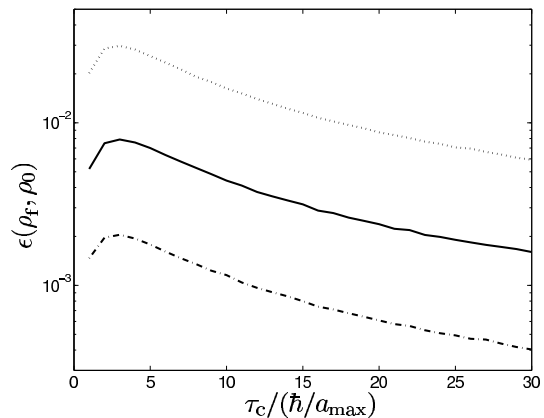


FIG. 3: Error $\epsilon(\rho_f, \rho_0) = 1 - \phi(\rho_f, \rho_0)$ of the GRAPE optimized pulse sequence, shown as a function of the correlation time τ_c for noise strengths $\Delta = 0.25 \times a_{\max}$ (dotted line), $\Delta = 0.125 \times a_{\max}$ (solid line), and $\Delta = 0.0625 \times a_{\max}$ (dash-dotted line).

B. One-qubit NOT gate

In this subsection, we analyze implementations of one-qubit NOT gates under RTN. The NOT gate corresponds to a π -rotation about the x -axis on the Bloch sphere and thus also carries out the bit flip considered in Sec. IV A. For quantum gate implementations, we use the fidelity function Φ defined in Eq. (11).

The π -pulse, CORPSE, and SCORPSE sequences are specifically designed to implement a NOT gate. However, the GRAPE pulse sequences for a bit flip and a NOT gate differ since the optimized fidelity functions are different for these two operations. Figure 4 shows the fidelities obtained with the π -pulse, CORPSE, SCORPSE, and GRAPE pulse sequences, as functions of the noise correlation time τ_c . The noise strength is set to be $\Delta = 0.125 \times a_{\max}$, as in Fig. 1. In comparison to the fidelities for the bit flip shown in Fig. 1, the fidelities for the NOT gate derived under the CORPSE and SCORPSE pulse sequences are lower, whereas the fidelity under the π -pulse is higher. Nevertheless, Figs. 1 and 4 show qualitatively the same phenomena, namely, motional narrowing in the short time correlation limit $\tau_c \rightarrow 0$ and correction of systematic errors in the long time correlation limit $\tau_c \rightarrow \infty$.

Since we employ the averaged gradient in Eq. (19) which effectively involves three gradients for fixed initial conditions, one might conclude that finding the optimized pulse sequences for quantum gates will require approximately three times as much computational time as for the bit flip. However, as noted above, the GRAPE algorithm finds the optimal operation time. This task is straightforward in the bit flip case, where as shown above, the fidelity is a monotonically increasing function of the operation time. For the NOT gate however, the optimization is nontrivial. Because of the averaging over initial conditions, the optimal fidelity does not necessar-

ily increase monotonically with T , as illustrated in Fig. 5. Finding the optimal operation time for a quantum gate thus clearly increases the complexity of the problem.

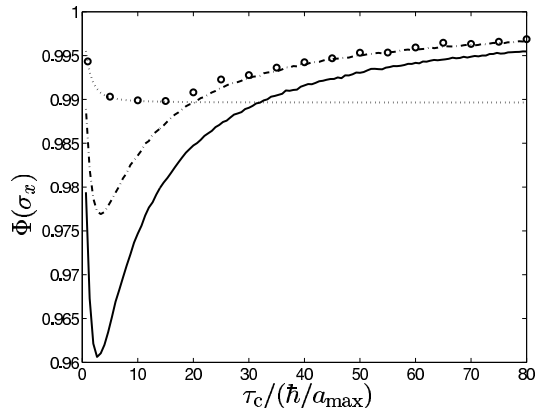


FIG. 4: Fidelities $\Phi(\sigma_x)$ for the NOT gate, shown as functions of the correlation time τ_c for a π -pulse (dotted line), CORPSE (solid line), and SCORPSE (dash-dotted line). The figure also shows the optimized fidelity found using the GRAPE algorithm (circles). The RTN strength Δ is set at $0.125 \times a_{\max}$.

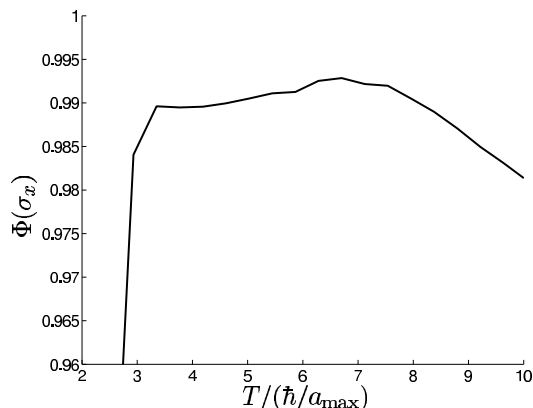


FIG. 5: Optimized fidelity $\Phi(\sigma_x)$ obtained from GRAPE, shown as a function of the operation time T for noise correlation time $\tau_c = 30\hbar/a_{\max}$ and noise strength $\Delta = 0.125 \times a_{\max}$.

Additional insight into the efficiency of the GRAPE pulse sequence may be obtained by examining the behavior of the optimal operation time as a function of the correlation time. As shown in Fig. 6, the optimal operation time of GRAPE increases sharply and approaches the time of the SCORPSE pulse sequence at a value $\tilde{\tau}_c \approx 18\hbar/a_{\max}$. The resulting fidelity also becomes very close to that obtained with SCORPSE, see Fig. 4. It appears from Fig. 4 that errors due to RTN cannot be efficiently corrected with bounded controls for correlation times shorter than $\tilde{\tau}_c$, and therefore the optimal operation time of GRAPE reduces to that of a π -pulse.

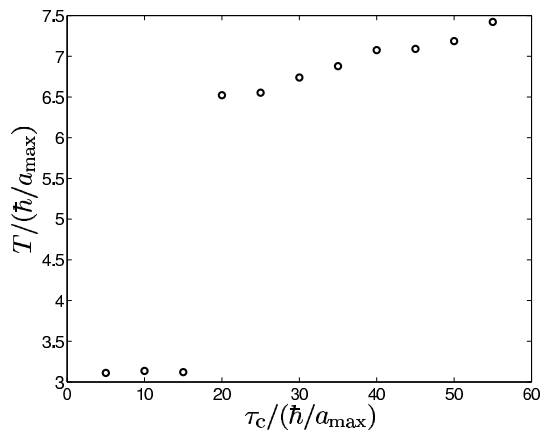


FIG. 6: Optimal operation time of pulse sequences obtained numerically with the GRAPE algorithm, shown as a function of the correlation time τ_c for noise strength $\Delta = 0.125 \times a_{\max}$.

V. CONCLUSIONS

In this work, we have studied how to perform high fidelity quantum operations on a one-qubit system that is subject to random telegraph noise acting on the qubit energy splitting. We considered examples of two major types of quantum operations, namely, a state transformation and a quantum gate. For the state transformation we chose a bit flip in which the one-qubit state is flipped from the south pole of the Bloch sphere to the north pole, whereas for the quantum gate we used the one-qubit NOT gate which generates a complete π -rotation on the Bloch sphere about the x -axis.

In both cases, we compared the fidelities obtained with the standard π -pulse, CORPSE, and SCORPSE pulse sequences. The same qualitative phenomena were obtained for all three types of pulse sequence. In the limit of vanishing correlation time, motional narrowing occurs and implies the π -pulse to be the most accurate sequence since it is time optimal in implementing the NOT gate or a bit flip. On the other hand, the CORPSE sequence yields the highest fidelity in the long correlation time limit $\tau_c \rightarrow \infty$, since it is designed to efficiently correct systematic errors. Over a rather wide intermediate range of the correlation time τ_c , SCORPSE yields the highest fidelity among all these three pulse sequences, suggesting that it may be a useful approach to suppress environmental noise in physical realizations of quantum computers.

Furthermore, we obtained fidelity optimized pulse sequences using the GRAPE algorithm which was always found to yield higher fidelities than the most accurate composite pulse sequence. Especially in the bit flip case, GRAPE yields noticeably higher fidelities than the composite pulse sequences. In contrast, GRAPE introduces only a rather marginal improvement over the most accurate composite pulse sequence for the implementation of the complete NOT gate.

The results of this paper provide useful bounds for the

implementation of high fidelity one-qubit operations in a noisy system without ancillary qubits. Although a simple RTN model is used in this paper, we expect that the qualitative dependency of the fidelity on noise strength and correlation time will also be present in a general qubit system. To investigate the validity of this conjecture, one may apply the methods presented here to the study of different noise models, e.g., Gaussian noise with a $1/f$ spectrum.

Other extensions of this work include high fidelity control of multi-qubit systems. Recent work has addressed optimal control of noiseless coupled superconducting qubits [27]. For these systems, the environmental noise may act on each qubit in either a correlated or uncorrelated fashion, which together with the entanglement of the qubits, expands the spectrum of the studies. It is an important open question to find a control sequence for the inter-qubit coupling term that implements a con-

trolled NOT gate with high fidelity in the presence of noise. To generalize the methods of this paper to noisy multi-qubit systems, a reformulation of the equations for the fidelity and its gradient is required.

Acknowledgments

We thank the NSF for financial support under ITR Grant No. EIA-0205641, and DARPA and ONR under Grant No. FDN0014-01-1-0826 of the DARPA SPINs program. MM acknowledges the Academy of Finland, the Finnish Cultural Foundation, and Jenny and Antti Wihuri's foundation for financial support. We would like to express our appreciation to S. J. Glaser and V. Shende for helpful discussions.

-
- [1] P. W. Shor, Phys. Rev. A **52**, 2493 (1995).
 - [2] A. M. Steanne, Phys. Rev. Lett. **77**, 793 (1996).
 - [3] P. Zanardi and M. Rasetti, Phys. Rev. Lett. **79**, 3306 (1997).
 - [4] D. A. Lidar, I. L. Chuang, and K. B. Whaley, Phys. Rev. Lett. **81**, 2594 (1998).
 - [5] E. Knill, R. Laflamme, and L. Viola, Phys. Rev. Lett. **84**, 2525 (2000).
 - [6] L. Viola and S. Lloyd, Phys. Rev. A **58**, 2733 (1998).
 - [7] L. Viola, S. Lloyd, and E. Knill, Phys. Rev. Lett. **83**, 4888 (1999).
 - [8] L. Viola and E. Knill, Phys. Rev. Lett. **90**, 037901 (2003).
 - [9] H. M. Wiseman, Phys. Rev. A **49**, 2133 (1994).
 - [10] H. M. Wiseman, Phys. Rev. A **50**, 4428 (1994).
 - [11] J. F. Poyatos, J. I. Cirac, and P. Zoller, Phys. Rev. Lett. **77**, 4728 (1996).
 - [12] T. D. Ladd, D. Mayenko, Y. Yamamoto, E. Abe, and K. M. Itoh, Phys. Rev. B **71**, 014401 (2005).
 - [13] Y. Nakamura, Y. A. Pashkin, T. Yamamoto, and J. S. Tsai, Phys. Rev. Lett. **88**, 047901 (2002).
 - [14] E. Collin, G. Ithier, A. Aassime, P. Joyez, D. Vion, and D. Esteve, Phys. Rev. Lett. **93**, 157005 (2004).
 - [15] N. G. van Kampen, *Stochastic Processes in Physics and Chemistry* (Elsevier, Amsterdam, 1992).
 - [16] S. Kogan, *Electronic noise and fluctuations in solids* (Cambridge University Press, Cambridge, 1996).
 - [17] T. Fujisawa and Y. Hirayama, Appl. Phys. Lett. **77**, 543 (2000).
 - [18] C. Kurdak, C.-J. Chen, D. C. Tsui, S. Parihar, L. S., and G. W. Weimann, Phys. Rev. B **56**, 9813 (1997).
 - [19] K. R. Brown, A. W. Harrow, and I. L. Chuang, Phys. Rev. A **70**, 052318 (2004).
 - [20] J. J. L. Morton, A. M. Tyryshkin, A. Ardavan, K. Porfyakis, S. A. Lyon, and G. A. D. Briggs, Phys. Rev. A **71**, 012332 (2005).
 - [21] H. K. Cummins and J. A. Jones, New J. Phys. **2**, 1 (2000).
 - [22] H. K. Cummins, G. Llewellyn, and J. A. Jones, Phys. Rev. A **67**, 042308 (2003).
 - [23] N. Khaneja, T. Reiss, C. Kehlet, T. Schulte-Herbrüggen, and S. J. Glaser, J. Magn. Reson. **172**, 296 (2005).
 - [24] M. A. Nielsen and I. L. Chuang, *Quantum Computation and Quantum Information* (Cambridge University Press, Cambridge, 2000).
 - [25] C. P. Slichter, *principles of magnetic resonance* (Springer-Verlag, Berlin, 1996).
 - [26] H. Geen and R. Freeman, J. Magn. Reson. **93**, 93 (1991).
 - [27] A. K. Spoerl, T. Schulte-Herbrüggen, S. J. Glaser, V. Bergholm, M. J. Storz, J. Ferber, and F. K. Wilhelm, quant-ph/0504202 (2005).